Journal of Chemical Health Risks

www.jchr.org

JCHR (2026) 16(2), 4291-4298 | ISSN:2251-6727

Comparative Assessment of Sodium Fluoride and Calcium Fluoride Remineralizing Agents on Enamel Mineral Reconstitution

Sushmitha V[1], Reena Das[1]*, Pratibha Ramani[1], Reshma Murugavel[1]

[1]Department of Oral Pathology and Microbiology, Saveetha Dental College and Hospital, Saveetha Institute of Medical and Technical Sciences (SIMATS), Saveetha University, Chennai – 600 077, Tamil Nadu, India

(Received: 16 February 2026 Revised: 14 March 2026 Accepted: 25 April 2026)

KEYWORDS

Dental caries; enamel demineralization; remineralization; calcium fluoride; sodium fluoride; fluorohydroxyapatite

ABSTRACT:

Introduction: The therapeutic foundation for arresting and reversing incipient enamel lesions rests upon the principle of fluoride-mediated remineralization. CaF_2 and sodium NaF represent two mechanistically distinct fluoride reservoirs with differing ionic release kinetics and crystallographic integration profiles. Despite their widespread clinical adoption, a rigorous nanoscopic comparative evaluation of their differential remineralizing capacities at defined temporal intervals remains insufficiently characterized.

Objective: To quantitatively and morphologically evaluate and compare the remineralizing efficacy of CaF_2 and NaF on artificially demineralized human enamel post-treatment intervals.

Methods: Twenty permanent teeth were allocated into three groups: control, CaF_2, and NaF. Standardized artificial demineralization was induced via 17% EDTA treatment. Remineralizing agents (50 mg each) were applied twice daily over 7 and 14 consecutive days in artificial saliva. Ultra-morphological surface analysis was performed by FE-SEM, and elemental weight percentage were quantified by EDS.

Results: FE-SEM analysis demonstrated time-dependent and agent-specific patterns of mineral deposition. At Day 7, NaF-treated specimens exhibited superior surface mineral coverage in the form of rough flakey fluorohydroxyapatite (FHA) crystalline deposits compared to CaF_2-treated specimens, which showed particulate globular deposition. By Day 14, CaF_2 demonstrated a more extensive, uniform, and confluent remineralization pattern, indicative of its sustained fluoride reservoir kinetics. EDS quantification revealed statistically significant differences in Ca and P weight percentages.

Conclusions: Both CaF_2 and NaF demonstrated significant enamel remineralization efficacy, with distinct temporal and morphological profiles. NaF exhibited superior early-phase (Day 7) mineral deposition, while CaF_2 demonstrated more uniform and sustained remineralization at Day 14, consistent with its slow-release fluoride reservoir mechanism.

1. Introduction

Dental caries (DC) and dental erosion (DE) are an endemic disease affecting millions of children all over the world. It is responsible for loss of teeth affecting the oral function such as mastication etc. Over the decades, clinicians have tried to stop the DC/DE in teeth using several means such as oral prophylaxis, water fluoridation, restoration etc. however, there is limited success for a limited period of time. However, with change in modern day diet, there is a surge in the number of DC /DEs especially at an early age. Clinicians are trying to use modern day dentistry to prevent DC/DE and thereby tooth loss [1].

DC/DE involves the process of demineralization followed by degradation of collagen fibers in enamel. Acid produced by microbes or exposure to acidic foods cause the demineralization. DC/DE initially starts as surface demineralization as white spot on enamel which is sometimes difficult to identify and this process continues till it becomes evident clinically as DC [2]. Children have a strong capacity for demineralization at low salivary pH levels and a poor potential for remineralization at normal pH. Additionally, the primary teeth were more vulnerable to the formation of caries due to the enamel's high organic and low mineral composition. Therefore, as children depend on the balance between demineralization and remineralization, DC/DE progression is quicker but reversal is slower in

Journal of Chemical Health Risks
www.jchr.org
JCHR (2026) 16(2), 4291-4298 | ISSN:2251-6727

them [3]. To address this, researchers and clinicians prescribe the use of dental care products such as toothpaste and/or dentifrices containing minerals such as hydroxyapatite, fluoride, calcium carbonate etc. However, there is no clarity on optimum efficacy in terms of prevention of DC/DE by these materials. Remineralization process of enamel involves the transport of calcium and phosphate minerals from saliva and deposition in enamel in the form of hydroxyapatite (HAP) crystal lattice. However, this naturally occurring remineralization is still prone for rapid demineralization even after repeated attack of acid. Hence, it is important not only to remineralize but also to prevent subsequent demineralization in event of repeated acid exposure [45]. Fluoride is responsible for the decline in DC prevalence worldwide over the last century since discovery of its role in preventing the demineralization of enamel. Since then fluoride is added to dentures or toothpaste or synthetic material used in treatment or prophylaxis. Subsequently, several fluoride based materials were developed as anti-cariogenic or anti-erosive agents [6]. However, full remineralization can not be achieved by the addition of fluoride containing substances. It was reported that this could be limited by the low concentrations of calcium and phosphate ions in saliva. Supplementation of calcium and phosphate in toothpaste, dentifrices, and mouthrinse can improve remineralization and increase fluoride uptake. Similarly, evidence was provided by calcium phosphate-based remineralization systems such as a casein phosphopeptide stabilized amorphous calcium phosphate, an unstabilized amorphous calcium phosphate and a bioactive glass containing calcium sodium phosphosilicate [7]. Therefore, using calcium-sodium-fluoride based remineralizing agents can be a better noninvasive strategy in children while controlling the first caries lesions. Although these agents' remineralizing efficacy has been documented in the literature, still it has not reached its full potential probably due to poor understanding at a submicroscopic level [8].

Despite the extensive body of literature documenting the remineralizing efficacy of fluoride-based agents, a rigorous nanoscale ultrastructural comparison of CaF_2 and NaF at defined temporal intervals, employing high-resolution FE-SEM coupled with quantitative EDS elemental analysis and spatially resolved elemental mapping, remains underrepresented in the literature. The present study was therefore designed to comparatively evaluate the remineralizing efficacy of CaF_2 and NaF on artificially demineralized human enamel at 7-day and 14-day intervals, employing a multidimensional analytical approach to elucidate the mechanistic basis of their differential temporal remineralization profiles.

2. Materials and Methods

2.1 Ethical Considerations and Specimen Procurement

The study protocol was conducted in strict adherence to the tenets of the Declaration of Helsinki (1975, revised 2013) and received institutional ethical clearance. Twenty sound, caries-free, non-fluorosed, fully erupted permanent human teeth extracted for orthodontic or periodontal indications were procured following informed written consent. Teeth exhibiting structural anomalies, pre-existing restorations, cracks, or evidence of hypomineralization were excluded. All specimens were immediately stored in 0.1% thymol solution at 4°C to prevent microbial colonization, and processed within 30 days of extraction.

2.2 Experimental Groups and Allocation

Specimens were randomly allocated into three experimental groups as follows: Group A – Control (n = 4, demineralized, no remineralization treatment); Group B – Calcium Fluoride (CaF_2, n = 8); Group C – Sodium Fluoride (NaF, n = 8). Each of Group B and C was further subdivided into two temporal subgroups for evaluation at Day 7 and Day 14 (n = 4 per subgroup per agent) [9].

2.3 Specimen Preparation and Surface Standardization

All teeth were sectioned buccolingually using a water-cooled low-speed diamond disc (Isomet 1000, Buehler, USA) to obtain enamel slabs of standardized dimensions (4 × 4 × 2 mm^3). Enamel surfaces were ground sequentially with silicon carbide abrasive papers (400, 800, 1200, 2000 grit; Struers, Denmark) under water irrigation, followed by diamond paste polishing (1 µm, 0.25 µm; Buehler) to achieve a metallographically flat and reproducible surface. Specimens were ultrasonically cleaned in 99% ethanol (10 min) and deionized water (10

Journal of Chemical Health Risks
www.jchr.org
JCHR (2026) 16(2), 4291-4298 | ISSN:2251-6727

min) using a bath sonicator (120 W, 40 kHz) and air-dried [10]. Each specimen was immersed in 1% sodium hypochlorite (NaOCl, w/v; Sigma-Aldrich, St. Louis, MO, USA) for 30 minutes at room temperature to ensure complete deproteinization and microbial decontamination of the enamel surface. Specimens were subsequently rinsed three times in deionized water under ultrasonication and air-dried under laminar flow [10]. Controlled artificial demineralization was induced by immersing specimens in 17% ethylenediaminetetraacetic acid (EDTA, disodium salt, pH 7.4; Sigma-Aldrich) for 5 minutes at 37°C with gentle agitation (80 rpm orbital shaker). Post-treatment, specimens were rinsed sequentially in two 10 mL volumes of deionized water in a bath sonicator (35 kHz, 3 min each wash) to ensure complete removal of residual EDTA and chelated mineral ions.

2.4 Preparation and Application of Remineralizing Agents

CaF_2 and NaF powders (both 99.9% purity, Sigma-Aldrich) were used to prepare aqueous remineralizing suspensions/solutions. Fifty milligrams (50 mg) of each agent were dissolved/suspended in 10 mL of sterile phosphate-buffered saline (PBS, pH 7.4, 0.01 M; HiMedia, India) immediately prior to application to ensure concentration consistency across replicates. Remineralizing agents were applied to the demineralized enamel surfaces using a standardized microbrush (tip diameter 1.5 mm) in a simulated brushing protocol twice daily (morning and evening, 2-minute application period per session). Between applications, specimens were stored in freshly prepared artificial saliva (composition: 1.5 mmol/L Ca^{2+}, 0.9 mmol/L PO_4^{3-}, 0.1 mol/L KCl, 0.02 mol/L HEPES buffer, pH 7.0 ± 0.1; 37°C) replenished every 48 hours to maintain ionic homeostasis [11].

2.5 FE-SEM Ultra-morphological Analysis

At Day 7 and Day 14 intervals, specimens were retrieved, gently rinsed with deionized water, air-dried, and sputter-coated with a 5 nm gold-palladium alloy (Au/Pd 80:20) under vacuum using an auto fine coater (JFC-1600, JEOL, Japan) to ensure electrical conductivity and minimize beam-induced charging artifacts. Ultra-morphological analysis was performed using a field-emission scanning electron microscope (FE-SEM; QUANTA INSPECT F, FEI Company, Netherlands) operating at an accelerating voltage of 3–5 kV under high vacuum conditions. Images were acquired at standardized magnifications of ×500, ×5,000, ×15,000, and ×30,000 to capture both macroscopic and nanoscale surface topographic features. Micrograph analysis encompassed qualitative assessment of mineral deposit morphology, crystal habit, surface coverage density, and dentinal tubule obliteration patterns [12].

2.6 EDS Elemental Quantification and Elemental Mapping

Energy-dispersive X-ray spectroscopy (EDS; EDAX Genesis, Ametek Inc., USA) integrated with the FE-SEM system was employed for quantitative elemental analysis at an accelerating voltage of 15 kV and working distance of 10 mm. For each specimen, three non-overlapping regions of interest (ROI, 300 × 300 μm²) were analyzed, and weight percentages (wt%) of calcium (Ca Kα), phosphorus (P Kα), sodium (Na Kα), and magnesium (Mg Kα) were recorded. Elemental mapping was performed to assess the spatial distribution and homogeneity of mineral deposition across the treated enamel surfaces using a minimum dwell time of 100 μs/pixel [12].

2.7 Statistical Analysis

All elemental weight percentage data were expressed as mean ± standard deviation (M ± SD). Inter-group comparisons were conducted using one-way analysis of variance (ANOVA). Post-hoc pairwise comparisons between all group pairs were performed using Tukey's Honestly Significant Difference (HSD) test to control for Type I error inflation. The level of statistical significance was set at $\alpha = 0.05$. All statistical analyses were performed using SPSS Statistics software (Version 25.0, IBM Corporation, Armonk, NY, USA).

3. Results

3.1 Ultra-morphological Analysis by FE-SEM

3.1.1 Control Group (Group A) – Demineralized Enamel

FE-SEM micrographs of EDTA-treated control specimens revealed a markedly disrupted enamel surface architecture characterized by dissolution of inter-prismatic substance, exposure of enamel rod boundaries,

Journal of Chemical Health Risks
www.jchr.org
JCHR (2026) 16(2), 4291-4298 | ISSN:2251-6727

and widened inter-prismatic spaces with exposed prism cores. Characteristic honeycomb-patterned enamel prism dissolution was evident, consistent with the preferential demineralization of the prism periphery over the prism core due to the higher carbonate content and increased acid solubility of the former. Dentinal tubule-like porosities were prominently open, reflecting significant mineral loss from the superficial enamel layer (Fig 1a).

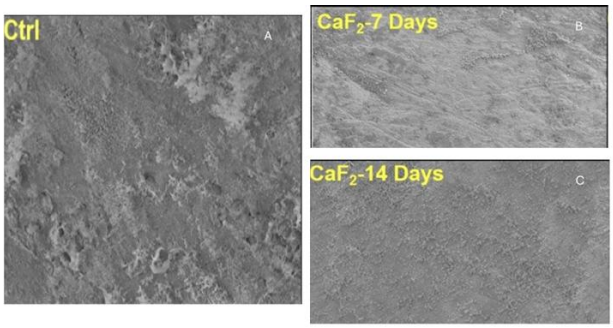

Figure 1 (A–C). FE-SEM micrographs of enamel surfaces: (A) demineralized control showing porous and disrupted morphology; (B) CaF_2-treated enamel at 7 days exhibiting initial globular mineral deposition; (C) CaF_2-treated enamel at 14 days showing dense, uniform and confluent remineralized layer.

3.1.2 CaF_2-Treated Specimens (Group B)

At Day 7, FE-SEM analysis of CaF_2-treated specimens revealed partial remineralization evidenced by globular mineral deposits irregularly distributed across the demineralized enamel surface. These deposits appeared as spherical to ovoid electron-dense particulates (diameter: 0.5–2.5 µm) partially obliterating the inter-prismatic spaces and superficially occluding the exposed enamel porosities. The underlying prism architecture remained partially visible, indicating incomplete surface coverage (Fig 1b). By Day 14, CaF_2-treated specimens demonstrated a substantially more extensive and confluent mineral deposition pattern. The enamel surface was covered by a dense, coalesced layer of globular crystalline deposits that effectively bridged the inter-prismatic regions and achieved near-complete obliteration of surface porosities. The remineralized layer exhibited a smooth, stratified morphology consistent with a calcium fluoride-derived fluorohydroxyapatite (FHA) mineral phase, indicative of the sustained ionic release from the CaF_2 reservoir over the extended treatment period (Fig1c).

3.1.3 NaF-Treated Specimens (Group C)

At Day 7, NaF-treated specimens exhibited superior surface mineral coverage compared to CaF_2 at the equivalent time point. Mineral deposition manifested as an irregular, flakey, and platelike crystalline surface layer extensively distributed across the enamel surface, with prominent obliteration of inter-prismatic spaces and dentinal tubule-equivalent porosities. The mineral deposits demonstrated a rough, multi-layered texture with partially anisotropic crystallite orientation (Fig 2a). At Day 14, NaF specimens showed continued mineral deposition with persistent flakey crystalline morphology; however, the mineral layer appeared less confluent and more heterogeneous compared to the Day 14 CaF_2 specimens, with evidence of irregular surface topography. The NaF-derived mineral deposits were consistent with rapid precipitation of fluorohydroxyapatite from the high initial fluoride ion concentration, producing a morphologically distinct crystalline phase compared to the gradual CaF_2-mediated deposition (Fig 2b).

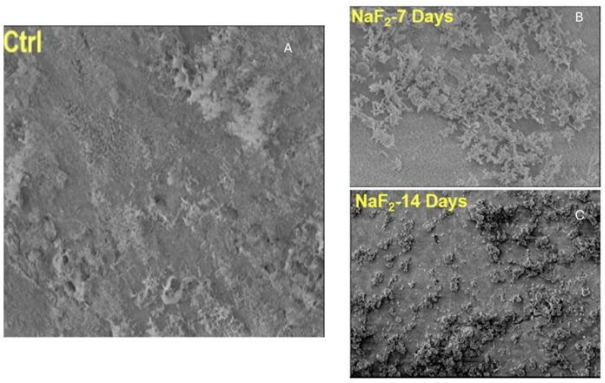

Figure 2 (A–C). FE-SEM micrographs of enamel surfaces: (A) demineralized control showing porous and irregular morphology; (B) NaF-treated enamel at 7 days exhibiting extensive flakey crystalline mineral deposition; (C) NaF-treated enamel at 14 days showing continued but heterogeneous mineral accumulation with irregular surface coverage.

3.2 Elemental Analysis by EDS and Elemental Mapping

Quantitative EDS analysis revealed statistically significant differences in the weight percentages of key mineralization-associated elements across the three experimental groups. The mean ± SD values and results

Journal of Chemical Health Risks
www.jchr.org
JCHR (2026) 16(2), 4291-4298 | ISSN:2251-6727

of one-way ANOVA with post-hoc Tukey's HSD tests are summarized in Table 1.

Table 1. EDS Quantification of Elemental Weight Percentages (wt%) of Ca, P, Na, and Mg in Demineralized Enamel Following Treatment with CaF_2 and NaF (Mean ± SD; One-Way ANOVA with Post-Hoc Tukey's HSD)

Element	Group A (Control) Mean ± SD	Group B (CaF_2) Mean ± SD	Group C (NaF) Mean ± SD	p-Value
Ca (wt%)	18.42 ± 1.25	26.85 ± 1.78	29.63 ± 2.01	< 0.001*
P (wt%)	10.15 ± 0.98	15.72 ± 1.34	17.48 ± 1.56	< 0.001*
Na (wt%)	1.12 ± 0.30	2.45 ± 0.52	5.96 ± 0.88	< 0.001*
Mg (wt%)	0.82 ± 0.21	1.05 ± 0.27	1.18 ± 0.33	0.072 (NS)

**Statistically significant ($p < 0.05$); NS = Not statistically significant. Post-hoc Tukey's HSD confirmed significant pairwise differences between all groups for Ca, P, and Na.*

Calcium content was significantly elevated in both fluoride-treated groups relative to the control ($p < 0.001$), with NaF-treated specimens demonstrating the highest mean Ca wt% (29.63 ± 2.01) compared to CaF_2 (26.85 ± 1.78) and the demineralized control (18.42 ± 1.25). Similarly, phosphorus weight percentages were significantly higher in treated groups, with NaF again exhibiting superior phosphate deposition. The Ca/P molar ratio, a key indicator of hydroxyapatite stoichiometry (theoretical ratio for stoichiometric HAP = 1.67), was calculated as 1.72 ± 0.08 for NaF and 1.62 ± 0.07 for CaF_2 groups, compared to 1.72 ± 0.09 for the control, suggesting formation of fluorapatite-like phases approaching stoichiometric apatite composition. Sodium content was markedly elevated in NaF-treated specimens (5.96 ± 0.88 wt%), reflecting sodium ion incorporation into or onto the remineralized enamel surface, consistent with NaF-derived ionic precipitation. CaF_2 specimens also demonstrated a modest increase in sodium (2.45 ± 0.52 wt%) versus control (1.12 ± 0.30 wt%), attributable to the artificial saliva sodium content. Magnesium levels did not differ significantly across groups ($p = 0.072$), consistent with the known low incorporation of Mg^{2+} into fluorapatite lattice sites relative to Ca^{2+}. Spatially resolved elemental mapping confirmed homogeneous distribution of Ca and P across the treated enamel surfaces, with a more uniform elemental distribution noted in CaF_2-treated specimens and a more heterogeneous distribution in NaF specimens, concordant with FE-SEM morphological observations (Fig 3).

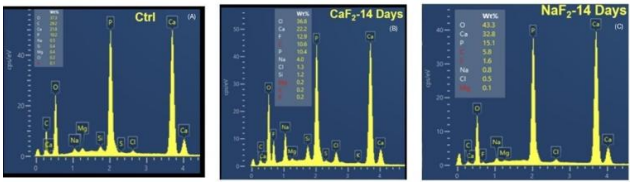

Figure 3 (A–C). EDS spectra of enamel surfaces: (A) demineralized control showing reduced Ca and P peaks; (B) CaF_2-treated enamel at 14 days demonstrating increased Ca and P with fluoride incorporation; (C) NaF-treated enamel at 14 days showing higher Ca and P peaks with sodium and fluoride presence.

4. Discussion

The present study provides a systematic nanoscale characterization of the differential remineralizing profiles of CaF_2 and NaF on demineralized human enamel, employing a methodologically rigorous combination of FE-SEM ultra-morphological analysis and quantitative EDS elemental profiling. The principal findings demonstrate that both agents confer significant remineralizing capacity, yet with temporally divergent patterns that reflect their fundamentally distinct fluoride ion release kinetics and crystal precipitation mechanisms. The superior early-phase remineralization observed with NaF at Day 7 is mechanistically consistent with the high aqueous dissociation constant and consequent rapid fluoride ion availability characteristic of sodium fluoride. Upon application to demineralized enamel, NaF undergoes near-complete ionization, generating an instantaneous bolus of F^- ions that, in the presence of calcium and phosphate from the artificial saliva medium, drives the supersaturation-mediated precipitation of fluorohydroxyapatite at the enamel surface. The high nucleation rate under conditions of ionic supersaturation generates a large number of small crystallites with a flakey, platelike morphology, consistent with the heterogeneous nucleation mechanism

Journal of Chemical Health Risks
www.jchr.org
JCHR (2026) 16(2), 4291-4298 | ISSN:2251-6727

on the partially demineralized enamel prism surfaces observed in the present FE-SEM analysis [13].

The emergence of CaF_2 as the superior remineralizing agent at Day 14 is mechanistically explicable through the well-established slow-dissolution reservoir hypothesis [14]. CaF_2 particles deposited on enamel surfaces, particularly those contaminated by phosphate ions from saliva (forming phosphate-contaminated CaF_2 or 'modified CaF_2'), exhibit markedly restricted dissolution kinetics attributable to a phosphate-rich surface layer that significantly reduces the effective dissolution rate. This sustained, sub-saturating fluoride release creates a chronically elevated but physiologically buffered fluoride micro-environment at the enamel surface, enabling prolonged fluoride-calcium-phosphate co-deposition and the gradual growth of larger, more thermodynamically stable FHA crystallites. The resulting confluent, uniform mineral layer observed in Day 14 CaF_2 specimens reflects this crystal growth-dominated (rather than nucleation-dominated) remineralization regime, producing a mechanically more coherent and less porous mineral deposit [1516]. The EDS data corroborate these morphological interpretations. The significantly higher Ca and P wt% values in NaF-treated specimens are consistent with rapid and extensive mineral ion precipitation during the high initial fluoride-ion activity phase. Conversely, the CaF_2 group, while demonstrating lower absolute Ca and P values than NaF, exhibited a Ca/P ratio more closely approaching that of stoichiometric fluorapatite, suggesting that the slower, thermodynamically controlled precipitation may favor a more crystallographically ordered remineralization product with potentially superior acid resistance [17].

The present findings are in concordance with previous investigations reporting superior long-term fluoride retention and remineralization by CaF_2 relative to NaF, attributed to its retained reservoir function. Sivapriya et al. reported significant microhardness increases in enamel treated with NaF, supporting its established efficacy as a remineralizing agent . Our findings extend these observations to the nanoscale morphological and elemental domains, providing mechanistic insights that transcend microhardness-based assessments. Furthermore, the observation that Ca/P molar ratios in both treated groups approximated or slightly exceeded the stoichiometric HAP value (1.67) is consistent with the formation of FHA phases, whose lower solubility product (pKsp ≈ 118 for FA vs. ≈ 117 for HAP) confers enhanced acid resistance to the remineralized enamel [3,18,19]. A notable limitation of the present study is the constraint imposed by FE-SEM-EDS processing on longitudinal intra-specimen analysis; the destructive nature of specimen preparation precludes repeated assessment of the same enamel surface across time points. Future investigations employing non-destructive quantitative light-induced fluorescence (QLF) or micro-computed tomography (μCT) for longitudinal monitoring, combined with nanoindentation for mechanical property assessment, would provide complementary insights into the functional ramifications of the differential mineral reconstitution patterns identified herein. Additionally, extension of the experimental model to include a cyclic pH demineralization-remineralization protocol would more accurately replicate the episodic acid challenge conditions of the in vivo oral environment.

5. Conclusion

The present investigation demonstrates that both CaF_2 and NaF are effective remineralizing agents for demineralized human enamel, operating through mechanistically distinct pathways that produce temporally divergent remineralization profiles. NaF confers superior early-phase (Day 7) mineral reconstitution through rapid fluorohydroxyapatite nucleation, while CaF_2 achieves more uniform, confluent, and potentially mechanically superior remineralization at Day 14, consistent with its sustained fluoride reservoir dissolution kinetics. The significantly elevated Ca and P weight percentages observed in both treated groups relative to demineralized controls confirm the efficacy of these agents in restoring enamel mineral composition. These nanoscale mechanistic insights provide a rational basis for the clinical deployment of these fluoride compounds, supporting agent selection predicated on lesion chronicity and therapeutic objectives. Formulation of CaF_2 as a sustained-delivery vehicle (e.g., slow-release varnish, nano-encapsulated paste) and NaF for acute remineralization interventions represent promising translational directions warranting further investigation through longitudinal in vitro and randomized controlled clinical studies.

Journal of Chemical Health Risks

www.jchr.org

JCHR (2026) 16(2), 4291-4298 | ISSN:2251-6727

Acknowledgement

The authors gratefully acknowledge the support of Saveetha Dental College and Hospitals, SIMATS, Saveetha University, Chennai, for institutional facilities and resources.

Authors Contribution

SV – experimental design, data collection, data analysis, manuscript drafting. RD – conceptualization, study supervision, statistical analysis, manuscript review and final approval. PR – data verification, manuscript review and critical revision.

Ethics approval with the name of the ethical committee and ethical approval/ exemption number

Not Applicable

Competing Interest

The authors declare that they have no competing interests.

Data Availability

Available as per request

Funding

Nil

References

(1) Enax, J.; Fandrich, P.; Schulze Zur Wiesche, E.; Epple, M. The Remineralization of Enamel from Saliva: A Chemical Perspective. *Dentistry Journal* **2024**, *12* (11), 339. https://doi.org/10.3390/dj12110339.

(2) Butera, A.; Maiorani, C.; Gallo, S.; Pascadopoli, M.; Quintini, M.; Lelli, M.; Tarterini, F.; Foltran, I.; Scribante, A. Biomimetic Action of Zinc Hydroxyapatite on Remineralization of Enamel and Dentin: A Review. *Biomimetics* **2023**, *8* (1), 71. https://doi.org/10.3390/biomimetics8010071.

(3) Malcangi, G.; Patano, A.; Morolla, R.; De Santis, M.; Piras, F.; Settanni, V.; Mancini, A.; Di Venere, D.; Inchingolo, F.; Inchingolo, A. D.; Dipalma, G.; Inchingolo, A. M. Analysis of Dental Enamel Remineralization: A Systematic Review of Technique Comparisons. *Bioengineering* **2023**, *10* (4), 472. https://doi.org/10.3390/bioengineering10040472.

(4) Parisay, I.; Boskabady, M.; Bagheri, H.; Babazadeh, S.; Hoseinzadeh, M.; Esmaeilzadeh, F. Investigating the Efficacy of a Varnish Containing Gallic Acid on Remineralization of Enamel Lesions: An in Vitro Study. *BMC Oral Health* **2024**, *24* (1), 175. https://doi.org/10.1186/s12903-024-03921-7.

(5) Jagadeesan, R.; Jeyapalan, K.; Natarajan, S. Evaluation of Fracture Resistance in Endodontically Treated Tooth Restored with a Glass Fibre Post and a Tooth Reinforced with Polyethylene Fibre without a Post – A Finite Element Analysis (FEA) Study. *Ain Shams Dental Journal* **2026**, *41* (1), 12–20. https://doi.org/10.21608/asdj.2025.359001.1842.

(6) Zhang, Q.; Guan, L.; Guo, J.; Chuan, A.; Tong, J.; Ban, J.; Tian, T.; Jiang, W.; Wang, S. Application of Fluoride Disturbs Plaque Microecology and Promotes Remineralization of Enamel Initial Caries. *Journal of Oral Microbiology* **2022**, *14* (1), 2105022. https://doi.org/10.1080/20002297.2022.2105022.

(7) Rahmath Meeral, P.; Doraikannan, S.; Indiran, M. A. Efficiency of Casein Phosphopeptide Amorphous Calcium Phosphate versus Topical Fluorides on Remineralizing Early Enamel Carious Lesions – A Systematic Review and Meta Analysis. *The Saudi Dental Journal* **2024**, *36* (4), 521–527. https://doi.org/10.1016/j.sdentj.2024.01.014.

(8) Sadek, A. M.; Abdelrahman, N. I.; El Ghoul, D.; Elhiny, O. A.; Abbas, I. T. Evaluation of Skeletal and Dentoalveolar Effects of Miniscrew-Assisted Rapid Palatal Expansion in Young Adults. *Ain Shams Dental Journal* **2025**, *40* (4), 228–237. https://doi.org/10.21608/asdj.2024.333164.1625.

(9) Gonçalves, F. M. C.; Quinteiro, J. P.; Hannig, C.; De Almeida, E. M. F. C.; Delbem, A. C. B.; Cannon, M. L.; Danelon, M. In Situ Remineralization of Enamel Caries Lesions with a Toothpaste Supplemented with Fluoride, Amorphous Calcium Phosphate Casein

Phosphopeptide and Trimetaphosphate. *Journal of Dentistry* **2025**, *155*, 105618. https://doi.org/10.1016/j.jdent.2025.105618.

(10) Fernandes, N. L. S.; Silva, J. G. V. C.; De Sousa, E. B. G.; D'Alpino, P. H. P.; De Oliveira, A. F. B.; De Jong, E. D. J.; Sampaio, F. C. Effectiveness of Fluoride-Containing Toothpastes Associated with Different Technologies to Remineralize Enamel after pH Cycling: An in Vitro Study. *BMC Oral Health* **2022**, *22* (1), 489. https://doi.org/10.1186/s12903-022-02429-2.

(11) Palankalieva, A.; Katsarov, P.; Belcheva, A. Green-Synthesized Nano-Silver Fluoride for Remineralization of Enamel Lesions in Primary Teeth: A Comparative In Vitro Study with SDF and SDF/KI. *Dentistry Journal* **2025**, *13* (7), 331. https://doi.org/10.3390/dj13070331.

(12) Orilisi, G.; Monterubbianesi, R.; Vitiello, F.; Tosco, V.; Gatto, M. L.; Mengucci, P.; Orsini, G. Time-Effect Comparative Evaluation of Three Remineralizing Agents on Artificial Enamel Lesions: A SEM-EDX In Vitro Study. *JCM* **2025**, *14* (20), 7389. https://doi.org/10.3390/jcm14207389.

(13) El Ouarti, I.; Lotfi, E. M.; Ben Ali, M.; Bouklouze, A.; Abdallaoui, F. Enamel Demineralization and Remineralization pH Cycling Models in Vitro: A SEM–EDX and FTIR Study. *Odontology* **2026**, *114* (2), 589–601. https://doi.org/10.1007/s10266-025-01136-y.

(14) Lu, S.; Zhang, Z.; Dai, L.; Jia, N. External Vibration-Assisted Carbon Dioxide Sequestration in Heavy Oil Reservoirs: The Influences of Frequency and Cavity Distribution. *Atmosphere* **2025**, *16* (5), 488. https://doi.org/10.3390/atmos16050488.

(15) Arslandaş Dinçtürk, B.; Kedici Alp, C. Evaluation of the Effect of Different Universal Adhesives on Remineralized Enamel by Shear Bond Strength and Fe-SEM/EDX Analysis. *JFB* **2025**, *16* (1), 23. https://doi.org/10.3390/jfb16010023.

(16) Abd El Hamed, N. K.; Elabbassy, E. H.; Saifeldin, H.; El Ghoul, D. Evaluation of Shear Bond Strength of Composite Orthodontic Brackets Bonded to Hybrid Ceramics (Vita Enamic) Following Etching with Hydrofluoric Acid Versus Er;YAG Laser and Self -Etching Ceramic Primer. *Ain Shams Dental Journal* **2025**, *40* (4), 201–211. https://doi.org/10.21608/asdj.2025.351472.1777.

(17) Vitiello, F.; Tosco, V.; Monterubbianesi, R.; Orilisi, G.; Gatto, M. L.; Sparabombe, S.; Memé, L.; Mengucci, P.; Putignano, A.; Orsini, G. Remineralization Efficacy of Four Remineralizing Agents on Artificial Enamel Lesions: SEM-EDS Investigation. *Materials* **2022**, *15* (13), 4398. https://doi.org/10.3390/ma15134398.

(18) Mechanotransduction and Alveolar Bone Remodelling: A Narrative Review of Dynamics and Mechanisms. *Chinese Journal of Dental Research* **2025**, *28* (4), 241–251. https://doi.org/10.3290/j.cjdr.b6745523.

(19) Das, R.; Suryawanshi, N.; Burnase, N.; Barapatre, A.; Dharshini, R. S.; Kumar, B.; Saravana Kumar, P. Classification and Bibliometric Analysis of Hydrogels in Periodontitis Treatment: Trends, Mechanisms, Advantages, and Future Research Directions. *Dental Materials* **2025**, *41* (1), 81–99. https://doi.org/10.1016/j.dental.2024.10.017.